

## Small veins of what diameters are visible in typical susceptibility weighted sequences?

Matthew P. Quinn<sup>1</sup>, and Ravi S. Menon<sup>1,2</sup>

<sup>1</sup>Medical Biophysics, The University of Western Ontario, London, Ontario, Canada, <sup>2</sup>Robarts Research Institute, London, Ontario, Canada

### INTRODUCTION

Evaluation of MR techniques that derive contrast from susceptibility benefits from the use of intricate phantoms with paramagnetic inclusions. To our knowledge no previous study has attempted to quantify the size of small veins to which susceptibility-weighted sequences are sensitive. Primary objectives of this study were to develop a phantom suitable for mimicking veins oriented perpendicular to  $B_0$  and with diameters less than the in-plane voxel dimension; and, to employ this phantom and a complementary computer simulation to estimate diameters of small veins visible in a frequency image generated from multi-echo gradient echo data.

### METHODS

**Phantom.** A phantom was created in a cylindrical container filled with agarose gel (1.0% w/v, 0.1 mM  $GdCl_3$ ), across the diameter of which a Teflon tube (ID/OD = 256/404  $\mu m$ ) was glued tautly in place. The tube was filled with gadolinium solution: the concentration chosen was 8.68 mM  $GdCl_3$  so that the dipolar field distribution outside the tube would be identical to that outside a vein of equal diameter. The phantom was scanned on a 3 T scanner with a 32-channel head coil, the tube oriented perpendicular to  $B_0$ . Multi-echo FLASH was employed with echoes from 10 to 45 ms with spacing of 7 ms. Acquisitions were performed with varying slice thicknesses but constant ratio of voxel dimensions (read : phase encode : slice = 1:1:2). A single frequency image was created for each acquisition by averaging the separate frequency images (i.e. homodyne filtered phase  $\div$  TE) of each echo.

**Simulation.** Voxel frequency was simulated for (i) a vein and (ii) the Teflon tube in the phantom described above, both oriented perpendicular to  $B_0$  and running through the center of a voxel. The simulation described in [1] was adapted: we used a two-compartment model for vein (inner, outer) and a three-compartment model for the tube (inner, annular, outer). The voxel was subdivided into many sub-voxels, in each of which the complex signal was determined numerically. Total voxel signal was the sum of all sub-voxel signals. This was performed at the same echo times as the acquisition above and a single frequency value was computed by averaging the phase  $\div$  TE from all echoes. This simulation was performed for vein and Teflon tube over a range of vessel diameters smaller than the voxel width. A constant ratio of inner to outer diameter was used for the Teflon tube simulation of 256/404.

**Human Data.** A healthy, 21 year-old female volunteer was scanned using the same multi-echo gradient echo sequence as above (axial acquisition, in-plane voxel size =  $0.5 \times 0.5$  mm<sup>2</sup>, slice thickness = 1.00 mm); a frequency map was generated in the same fashion.

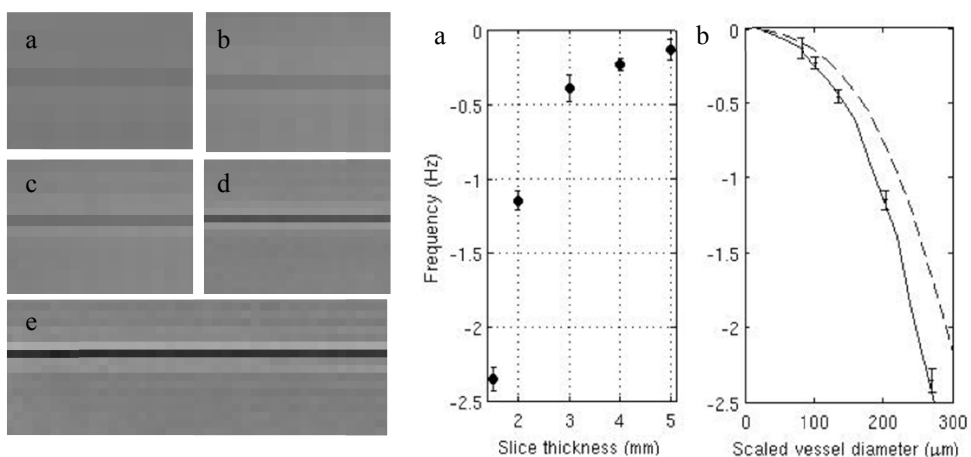
### RESULTS & DISCUSSION

Representative frequency images of the phantom for different acquisitions/voxel sizes are presented (Fig. 1). Effectively, decreasing voxel size for constant tube diameter is equivalent to increasing vein diameter for a constant voxel size. Frequency was measured for each acquisition as the mean value in a region of interest placed within the row of voxels containing the tube. These values are plotted against true slice thickness (Fig. 2a) and against tube diameter normalized by the acquisition slice thickness and multiplied by a nominal slice thickness of 1 mm (Fig. 2b). Simulation results for the Teflon tube and vein are also plotted as curves (Fig. 2b), where strong agreement is seen between simulation and *in vitro* values for Teflon tube. Discrepancy between simulation values for vein and tube is attributed to differences in intra-vessel field. While the extra-vessel fields are nearly identical, the intra-vessel field shift is much larger for the Teflon tube: this is due to the relatively high gadolinium concentration required within the tube to overcome the Teflon's diamagnetic susceptibility. Frequency measured in small periventricular veins *in vivo* was  $-0.75 \pm 0.31$  Hz. Interpolating from simulation, this corresponds to diameters ranging from 160 to 230  $\mu m$ , which is less than half the in-plane dimension.

#### Fig. 1 Frequency images of phantom

(left). Slice thicknesses are, from (a) to (e): 5, 4, 3, 2, and 1.5 mm. All images are windowed from -4 to +4 Hz.

**Fig. 2 Frequency plots (right).** The values of frequency measured in phantom are plotted in (a) against true slice thickness; this same data is re-plotted in (b) against tube diameter scaled by acquisition slice thickness and multiplied by a slice thickness of 1 mm. Also in (b) are simulated frequency data for the Teflon tube in agarose (solid line) as well as a vein (dashed line).



### CONCLUSION

Small veins with diameters on the order of 200  $\mu m$  are visible in frequency images with the typical resolutions of  $0.5 \times 0.5 \times 1.0$  mm<sup>3</sup> used in susceptibility-weighted imaging sequences. To our knowledge, this is the first attempt to quantify diameters of small veins visible with susceptibility-weighted sequences.

**REFERENCES** [1] Xu and Haacke Magn. Reson. Imaging 2006; 24:155-160.